13th World Conference on Earthquake Engineering
Vancouver, B.C., Canada
August 1-6, 2004
Paper No. 1174

SEISMIC SAFETY EVALUATION OF BASE-ISOLATED HOUSES WITH RUBBER BEARING

Masanori IIBA[1], Mitsumasa MIDORIKAWA[2], Hiroshi HAMADA[3], Yoshinobu YASUI[4] and Tsutomu HANAI[5]

SUMMARY

The structural safety of seismically isolated houses is focused, when a collision of isolated interface will occur against very severe earthquakes with a long period component. Shaking table tests are carried out to investigate the responses of a seismically isolated system with rubber bearings for houses and to verify effects of displacement restraint device made by rubber material. A numerical analysis on earthquake response of base-isolated houses with displacement restraint device is conducted. Through effects of the device on story drift response of superstructures, the structural safety of superstructures during the collision of isolated interface is discussed.

INTRODUCTION

In order to apply seismically base-isolated systems to houses, not only the development of isolators for light-weighted superstructures but also the investigation of seismic behavior is needed (Iiba, et al. [1, 2], Myslimaj, et al. [3]). In case of light structures such as steel and timber houses, the buckling of rubber bearing isolators will easily occur because of slender-shaped isolators which provide the isolated systems with a long period. Measures to prevent isolators from buckling should be considered and verified.

It is desirable that the horizontal displacement response of the isolated interface during earthquakes is less than the buckling displacement. When a clearance of superstructure and peripheral retaining wall is small, a collision of them probably occurs. In this case, the effects on the response of superstructures or the validity of displacement restraint systems at isolated interface have to be clarified.

Shaking table tests are conducted to investigate the responses of a seismically isolated system with rubber bearings for houses and to verify the effect of displacement restraint device made by rubber material (Iiba, et al. [4]). To improve the stability of horizontal load-bearing capacity against buckling in rubber bearing

[1] Research Coordinator for Advanced Building Technology, National Institute for Land and Infrastructure Management, Japan, iiba-m92hx@nilim.go.jp
[2] Research Coordinator for Building Technology, Building Research Institute, Japan, midori@kenken.go.jp
[3] President, Hamada Techno-consultants, Japan, hiro7@fine.ocn.ne.jp
[4] Design Engineer, Kinugawa Rubber Industrial Co., Ltd., Japan, yoshinobu.yasui@kinugawa-rubber.co.jp
[5] Director, Nihon System Sekkei Co., Ltd., Japan, hanai@nittem.co.jp

isolators, steel plates with partially sharing vertical load are incorporated. Also the displacement restraint device with displacement-hardening type is set to control shock responses against collisions. Acceleration and displacement responses of the seismically isolated model subjected to three dimensional earthquake motions were measured. Based on experimental results, the effects of buckling protecting plates and displacement restraint devices on the response of isolators are evaluated.

In addition, a numerical analysis on earthquake response of base-isolated houses with displacement restraint devices is conducted. Through effects of displacement restraint devices on story drift responses at first story, the structural safety of superstructures during the collision of isolated interface is discussed.

SHAKING TABLE TESTS OF SEISMICALLY ISOLATED MODEL

Seismically isolated model

The seismically isolated model is set on a shaking table, as shown in Fig. 1. The isolated model is composed of 6 isolators, 4 hydraulic dampers and a mass supported by them. The dimension of the mass is 5.64 and 2.82 m in longitudinal and transverse directions, respectively. The mass with about 15.9 ton is made of a frame of H-shaped steel (H-250x250x9x14), square-sectional steel pipes whose hollow parts are filled with lead, and 4 steel plates on the H-shaped steel frame.

The outline of isolators is illustrated in Fig. 2. Values of equivalent stiffness and viscous damping ratio are design ones. To improve the stability against buckling, steel plates, which prevent isolators from buckling, are added, as shown in Fig. 2 and Photo 1. Relationships between shear force and horizontal displacement of isolators with/without buckling protecting plates are drawn in Fig. 3. And Fig. 4 presents equivalent stiffness and viscous damping ratio of isolators in two cases. The load-bearing capacity of isolator without

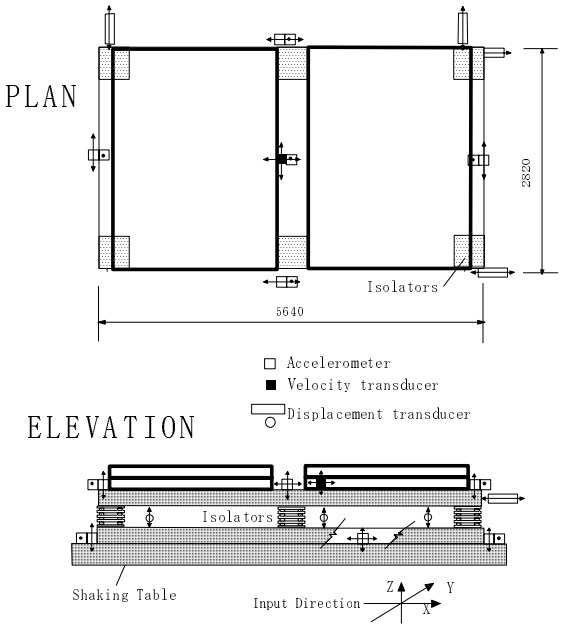

Fig. 1 Outline of seismically isolated model
(↔: parallel to sheet plane)

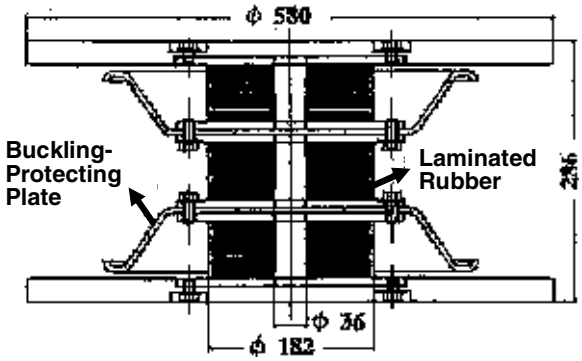

a) High damping rubber
b) 3 rubber bearings in series
c) Vertical loading capacity: 90kN.
d) Horizontal displacement limit: 250mm
e) Equivalent stiffness at displacement of 180mm: 24.2kN/m
f) Equivalent viscous damping ratio: about 10%

Fig. 2 Isolators (Elastomeric type)

Photo 1 Isolator with buckling protecting plate

plates little increases under the amplitude of horizontal displacement more than 100 mm. The equivalent stiffness is lower with displacement, and the equivalent viscous damping ratio is larger. It is found out that the characteristics of isolator without plates are much dependent on horizontal displacement. On the other hand, the isolator with plates has very stable characteristics with horizontal displacement.

The damping ratio of about 10 % in isolators is not enough to control the horizontal displacement of isolated interface. In the shaking table test, hydraulic dampers are installed to keep the equivalent viscous damping ratio of total 35% in the seismically isolated model.

Displacement restraint device

The displacement restraint device shown in Photo 2 is used in the test to control the displacement of isolated interface. Purposes of installing the device are to protect isolators from large displacement response and to mitigate large shock due to collision during very severe earthquakes. The device is made of 16 pieces of rubber which shape is like shell. The relationship between load and displacement of the device in static condition is shown in Fig. 5. The load-carrying capacity increases with displacement. In the experiment, when the isolated displacement reaches 150 mm, the device becomes effective, that is, the tips of rubber contacts

Photo 2 Displacement restraint device

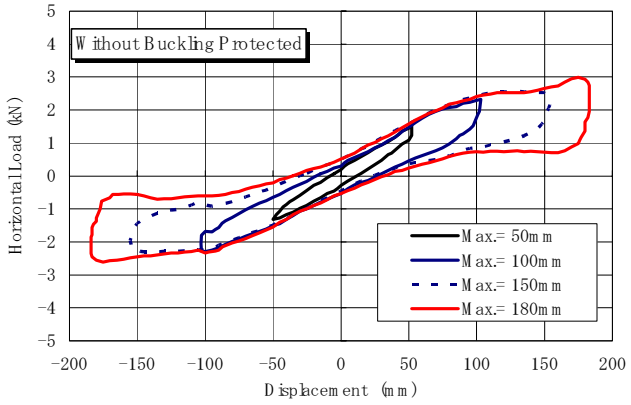

a) Without buckling protecting plate

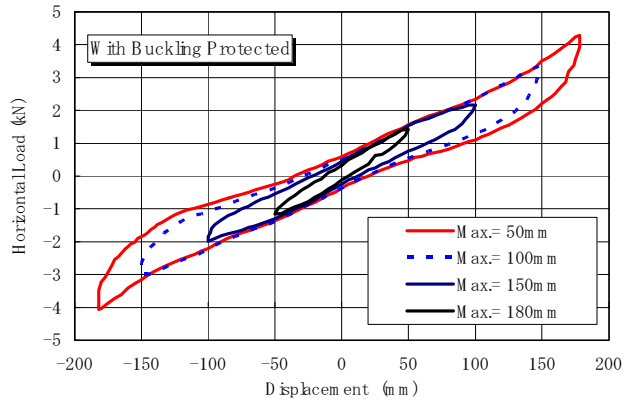

b) With buckling protecting plate

Fig.3 Relationship between shear force and horizontal displacement of isolators

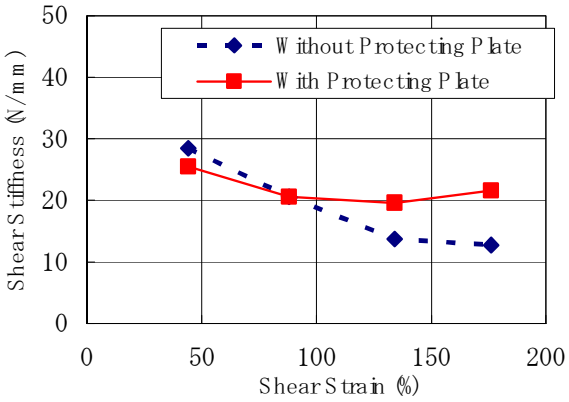

a) Equivalent stiffness

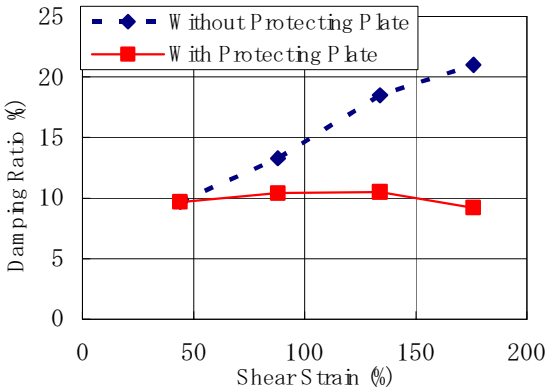

b) Equivalent damping ratio

Fig.4 Effect of buckling protecting plate

with circular steel plate (refer to Photo 2).

Measurement and earthquake motion

The arrangement of instruments in the seismically isolated model is presented in Fig. 1. Accelerations and velocities of table and isolated mass, horizontal and vertical displacements of isolated interface are mainly measured. The accelerometers with strain gauge type, velocity transducers with servo type and displacement transducers with laser, linearly pulse-count type, etc. are used.

In the test, the earthquake motion which was observed at Japan Meteorological Agency of Kobe city (JMA Kobe) in 1995 Hyogoken Nanbu earthquake is adopted by maximum velocity. The amplitude of the earthquake motion is adjusted. For example, the earthquake of 50 cm/s means that maximum velocity of NS component is 50 cm/s and other components are proportional to the NS one.

Table 1 presents examples of maximum velocities of earthquake motions at the shaking table. The combination of excited axes is shown in Table 2. One (X or Y directions), two (X and Y, simultaneously) and three dimensional earthquake motions are used. X, Y and Z directions are corresponding to EW, NS and UD components of observed earthquake motions.

High frequency components of measured acceleration data are removed through low pass filter. Fourier spectra of acceleration data, which are multiplied by a function of decreasing from 1 to zero with frequencies of 15 to 20 Hz, are converted to time histories. Velocity and displacement data are not filtered.

RESULTS OF SHAKING TABLE TEST

Behaviors of seismically isolated model

Time histories of response of seismically isolated model against one dimensional (Y-direction) earthquake motion with velocity of 50 cm/s are drawn in Fig. 6. The amplitude of maximum acceleration at table level and isolated interface are 484 and 121 cm/s^2, respectively. The amplitude of acceleration at isolated interface is about 0.25 times of that at table due to isolation. The time histories of acceleration and

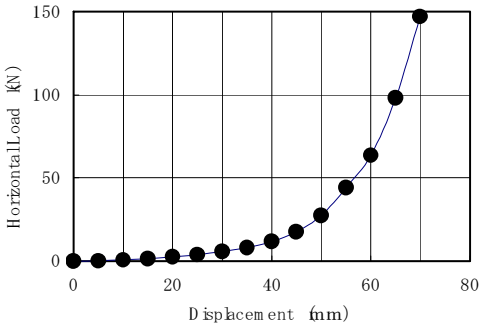

Fig.5 Characteristics of displacement restraint device

Table 1 Example of maximum velocities of earthquake motions

Max. Velocity (cm/s)	Direction		
	X	Y	Z
50	44.6	48.3	23.1
90	81.6	88.9	39.6

Table 2 Series of excitation by number of axes

Number of input axis	X (EW-comp)	Y (NS-comp)	Z (UD-comp)
One (X)	O		
One (Y)	O		
Two (XY)	O	O	
Three (XYZ)	O	O	O

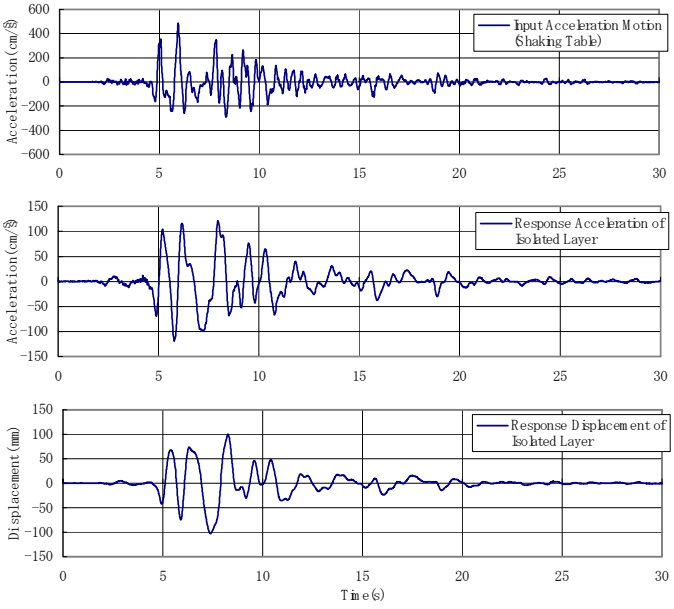

Fig. 6 Time histories of response of seismically isolated model (Y-direction)

displacement at isolated interface contain the response with long period during main excitation.

Relationships between shear coefficient and displacement of isolated interface are shown in Fig. 7. The figure compares among the relationships in Y direction against Y, XY and XYZ earthquake motions. The relationships under two- and three-dimensional motions are similar to that under one-dimensional motion except including high frequency response in shear coefficient. The effect of two dimensional and vertical motions on the response of isolated model is not remarkable, as the Y axis (NS component) is main one in 1995 JMA Kobe earthquake.

Figure 8 presents maximum response of isolated interface with maximum acceleration of earthquake motions. The horizontal responses of acceleration and displacement increase with input acceleration. The

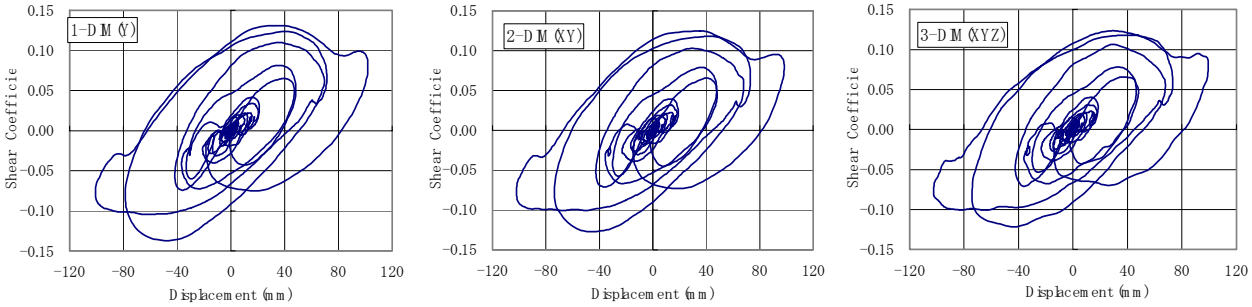

Fig. 7 Relationships between shear coefficient and displacement of isolated interface

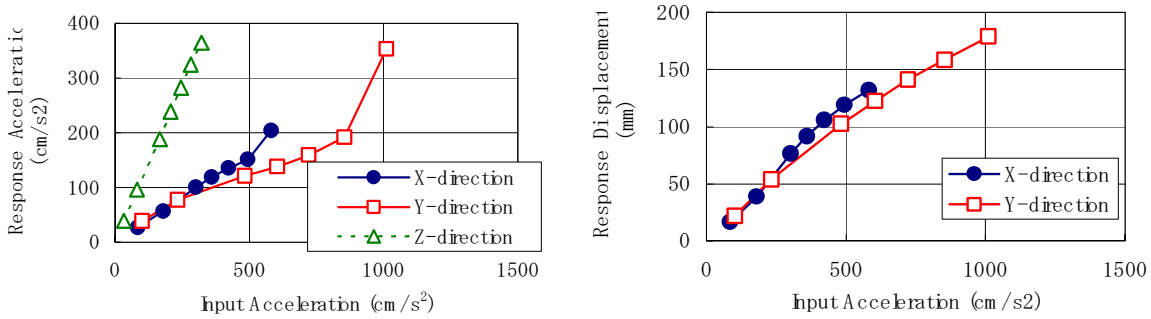

a) Maximum acceleration b) Maximum displacement

Fig. 8 Maximum response of isolated interface with earthquake motions

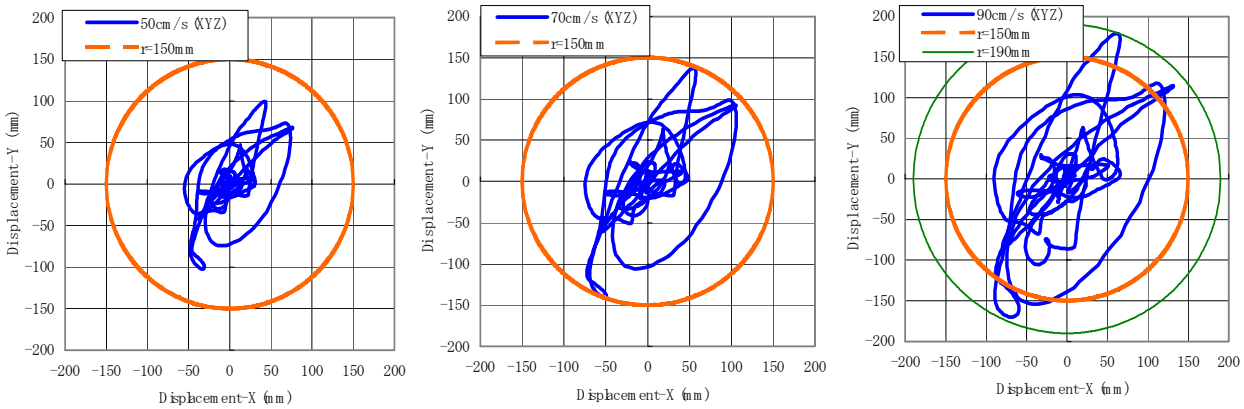

Fig. 9 Displacement orbits of isolated interface

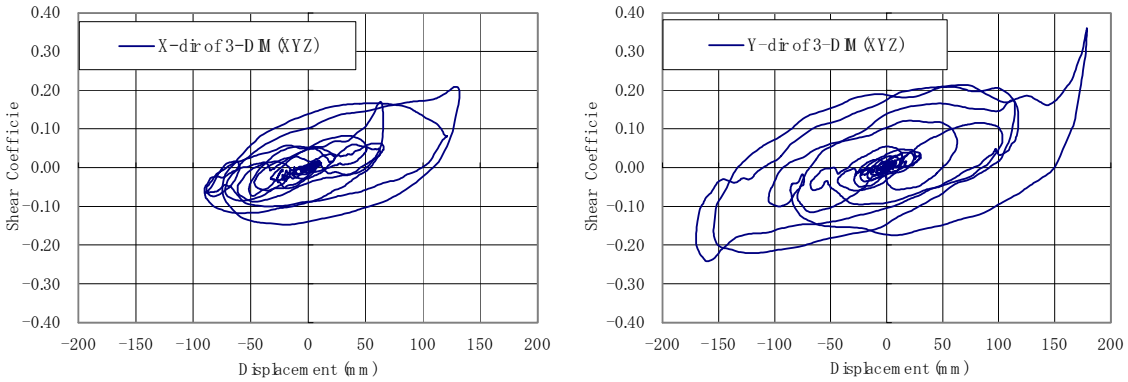

Fig. 10 Shear coefficient vs. displacement of isolated interface with 90 cm/s earthquake motion

acceleration responses remarkably increase with large input acceleration because the displacement restraint device is operational and the collision occurs at isolated interface. The vertical response accelerations are a little larger than input accelerations. The displacement orbits of isolated interface with three levels of XYZ-earthquake motions are drawn in Fig. 9. The displacement restraint device is set to be operational at the displacement of isolated interface of more than 150 mm. Under the earthquake motion with maximum velocity of 70 cm/s, the displacement reaches 150 mm. In case of the earthquake with 90 cm/s of velocity, the displacement of restraint device is about 40 mm.

Figure 10 presents the shear coefficient vs. displacement in X and Y directions at isolated interface with 90 cm/s XYZ-earthquake motion. The collision occurs at five times referring to the displacement orbit as shown in Fig. 9. At one of them, the shear coefficient in Y-direction is quite large.

SIMULATION ANALYSIS OF SEISMICALLY ISOLATED MODEL

The time history analysis is conducted using one degree of freedom system to simulate the experimental results of seismically isolated model. As the analysis covers the one-dimensional system, let us calculate the response in a principle axis which is defined to provide maximum response displacement in XY plane. Table 3 summarizes angles of principle axis to X-axis in deferent earthquake motions. The angles are almost constant by around 70 degree to the X-axis. Table 4 shows the analytical values of the seismically isolated model in the test. The characteristics of displacement restraint device are modeled to an approximated function as shown in Fig. 11.

Table 3 Angles of principle axis

Max. Velocity (cm/s)	Angle (degree)
50	66.6
60	-109.9
70	-110.6
80	-111.5
90	70.4

The simulation result of response in the case with maximum velocity of 50 cm/s is compared with the experimental one in Fig. 12. The accelerations and

Table 4 Values for analysis for seismically isolated model

Item	Unit	Value
Mass	t	16.0
Stiffness	kN/m	150
Damping ratio	-	0.35

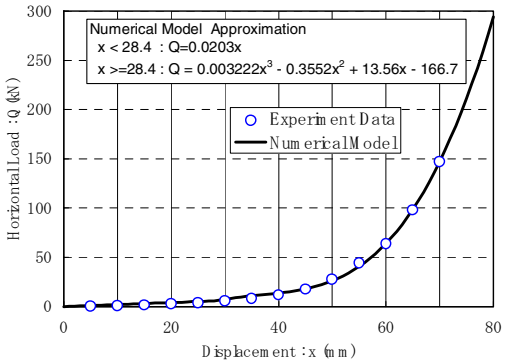

Fig. 11 Model of displacement restraint device

displacements in X and Y directions are converted to those in the principle axis. The simulated result has a good agreement with that in the experiment. Figure 13 presents the comparison between numerical and experimental results in case with maximum velocity of 90 cm/s. Under the earthquake motion, the collision occurs in several times. The shear coefficient of isolated interface at the collision in the analysis is a little larger than that in the experiment. Because it seems that the hysteretic damping of displacement restraint device is neglected in the analysis.

SAFETY EVALUATION OF SEISMICALLY ISOLATED HOUSES UNDER COLLISION

Based on the calculation results of seismically isolated houses with displacement restraint devices during earthquakes, the effects of the collision at isolated interface on the seismic safety of superstructure are investigated.

Setting of numerical model

The seismically isolated houses with general 2-story steel in superstructure are analyzed. The model of isolated interface is a combination of a linear spring and a dashpot. The natural period of isolated model is set to be 3.0 s and the damping ratio is supposed to be 35 %.

The same displacement restraint device used in the experiment is used at isolated interface. The characteristics of the displacement restraint device are that the shear force of 150 kN reacts at the horizontal displacement of 70 mm as shown in Fig. 11.

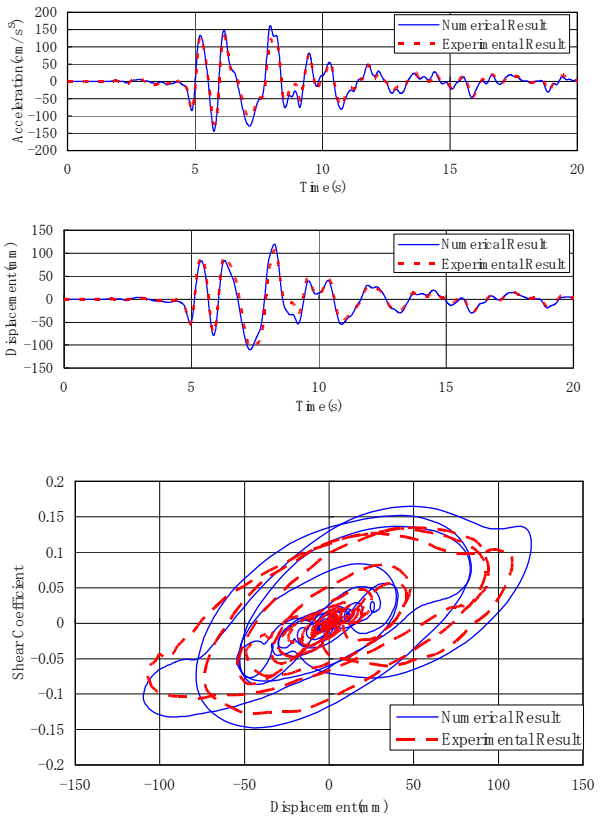

Fig. 12 Numerical results compared with experimental ones (Max. velocity 50cm/s)

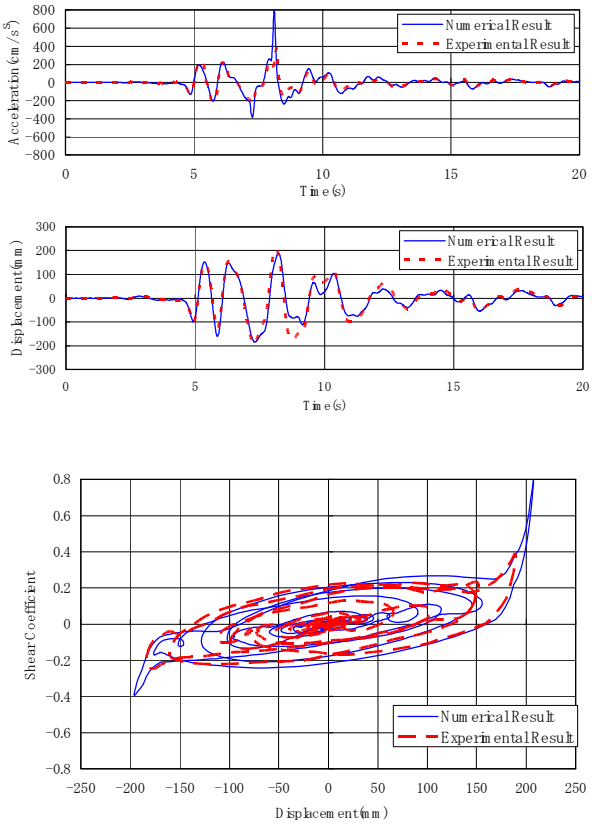

Fig. 13 Numerical results compared with experimental ones (Max. velocity 90cm/s)

The superstructure, whose total mass is around 60 t, have a mass distribution of 1.0, 1.0 and 0.75 at 1st, 2nd and roof floor levels, respectively, as illustrated in Fig. 14. The relationship between shear force and story drift at 1st story of superstructure is modeled to be a tri-linear one, as shown in Fig. 15. The story drifts of primary and secondary yielding points are assumed to be H/200 and H/75 (H: story height), respectively. The ratio of shear force to weight in upper part of the story at primary yielding point is 0.2. The secondary and third stiffness are 0.4 and 0.05 times of primary stiffness, respectively. The primary stiffness distribution of superstructure is set to be a linear distribution of displacement through the height. The stiffness at second story is 0.65 times of that at first story. And the viscous damping ratio is 3 % at the natural frequency and proportional to the stiffness. The ultimate story drift of superstructure is assumed to be H/20.

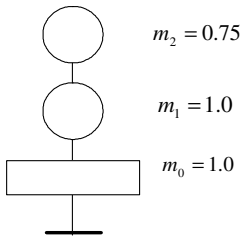

Fig. 14 Mass distribution of model

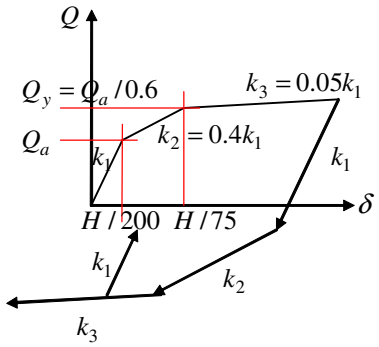

Fig. 15 Relationship between shear force and story drift

Earthquake motions

In the analysis, following earthquake motions are considered;

a) Simulated earthquake motions

Simulated earthquake waves at ground surface are calculated based on the acceleration response spectrum at outcropped engineering bedrock and wave amplification of surface ground layer. As earthquake motions at the outcropped engineering bedrock, ten wave forms with random phase and 60 s in length based on the acceleration response spectrum, which is 800 cm/s^2 of acceleration in short period (less than 0.64 s) and 82.5 cm/s of velocity in long period (5 % damping ratio) (Midorikawa, et al. [5]), are calculated. The acceleration time histories at ground surface are obtained through equivalent linear procedure (Yoshida, et al. [6]). Two sites with different ground conditions are selected. One is a medium soil ground with predominant period of 0.32 s and the other is softer with that of 0.48 s. As nonlinear characteristics of soil, the relationship proposed by Ohsaki et al. [7] is adopted. Figure 16 presents the pseudo velocity response spectra (average of 10 waves) at two sites compared with those of earthquake motions observed at JMA Kobe in 1995 hyogoken Nanbu Earthquake.

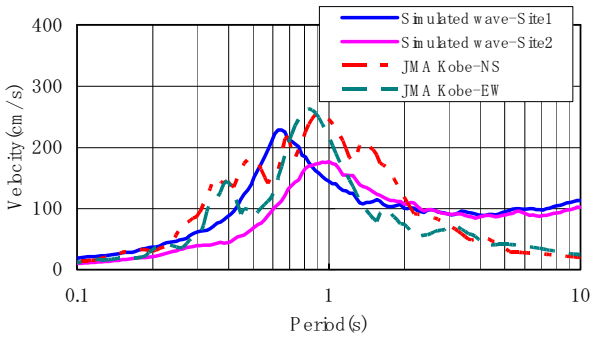

Fig. 16 Pseudo velocity response spectra of simulated earthquake motions

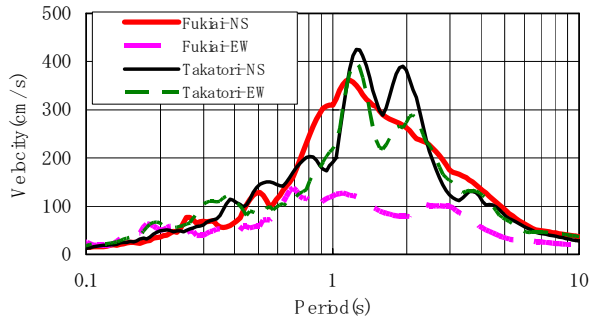

Fig. 17 Pseudo velocity response spectra of earthquake motions at Fukiai and Takatori

b) Observed earthquake motions

The earthquake motions named Fukiai (EW component) and Takatori (NS and EW

components) whose acceleration data are observed in 1995 hyogoken Nanbu Earthquake are adopted. As shown in Fig. 17, the pseudo velocity responses of these earthquake motions are larger than those at JMA. It is estimated that the horizontal displacement responses at isolated interface do not exceed 250 mm, where the collision will start, under the earthquake motions of JMA and NS component of Takatori.

Parameters of analysis

In the analysis, following parameters are considered;

a) Superstructure

Bearing capacities (shear strength) of stories are three kinds, that is, standard (above-mentioned), 1.25 and 1.5 times. And the viscous damping ratios are 3 (standard), 6 and 9 %.

b) Amplitude of earthquake motions

In case of isolated houses subjected to simulated earthquake motions, the amplitudes of maximum acceleration are enlarged by 1.0 to 3.0 times with step 0.1. After time history analysis is conducted against ten simulated earthquake motions, average value is calculated and plotted.

c) Operation point of displacement restraint device

In case of isolated houses subjected to simulated earthquake motions, operation points of displacement restraint device are set to be 200 and 250 mm.

In case of isolated houses subjected to observed earthquake motions of Fukiai and Takatori, the operation points vary from 250 to 450 mm with step 50 mm.

d) Number of displacement restraint device

The numbers of displacement restraint device are 2 or 4.

Results of analysis

Since the results of response in case of 2 and 4 displacement restraint devices are almost same, the results in case of 2 sets of displacement restraint devices are plotted in the following.

The results of analysis on the standard model with operation point of 200 mm, subjected to 2.0 times of simulated earthquake motions at site 2 are shown in Fig. 18. The relationships between shear force and horizontal displacement at isolated, 1st and 2nd stories and time history of acceleration response at isolated floor are drawn. The impulsive accelerations occur at stages of collisions at isolated interface. With

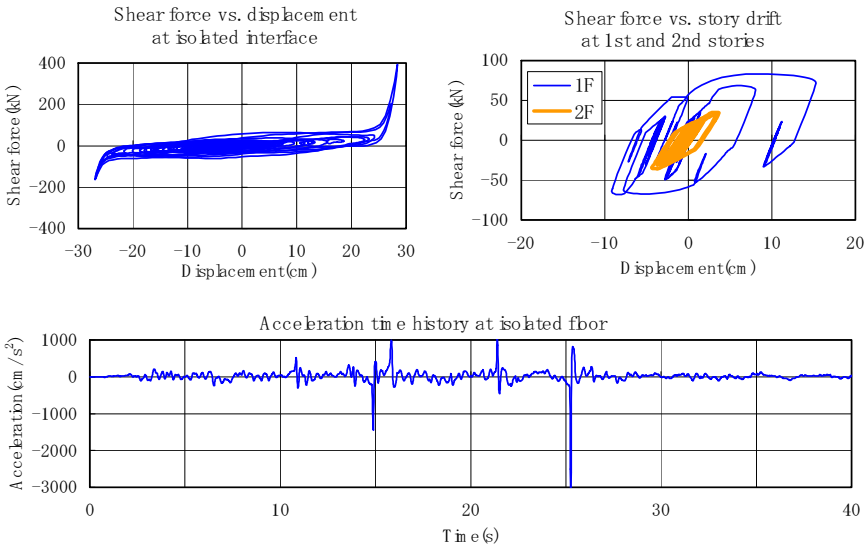

Fig. 18 Results of analysis on standard model

large accelerations, shear force of 1st story increases and the large hysteretic loop is observed.

The analytical results are arranged by following two factors.

a) Maximum of velocities of isolated interface at the operation points (Vop)

b) Difference between maximum displacement without displacement restraint device and operation point, i.e., controlled displacement (Dcon)

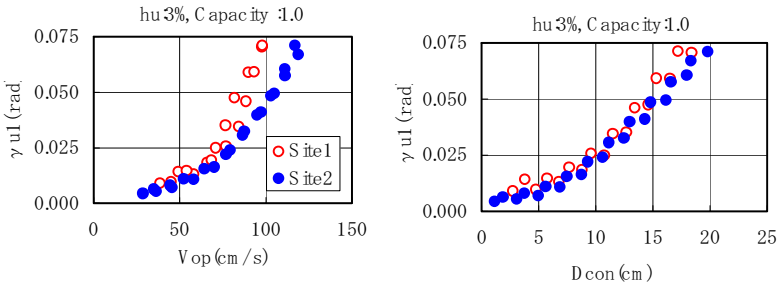

Fig. 19 Maximum drift angle of 1st story (γ_{u1}) with Vop or Dcon against simulated earthquake motions

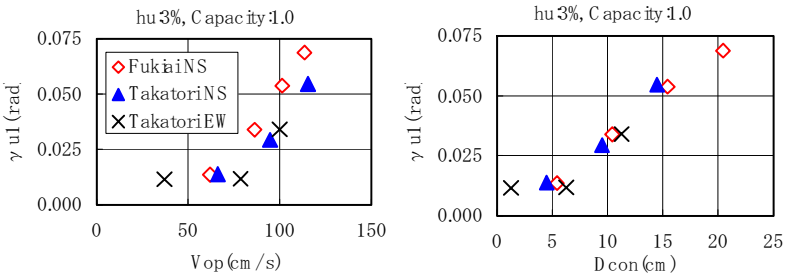

Fig. 20 Maximum drift angle of 1st story (γ_{u1}) with Vop or Dcon against observed earthquake motions

Figure 19 presents the maximum responses of drift angle at 1st story (γ_{u1}) with Vop or Dcon during simulated earthquake motions with different amplitude. The story drift angles remarkably increase with amplitude of Vop or Dcon. As to Vop, the story drift angles in case of site1 are larger than those in site2. Because during operating displacement restraint device, the superstructure is excited under base fixed condition (without isolation) and the predominant period of the superstructure is very similar to that in the earthquake motion at the site1. As to Dcon, the difference between the site conditions is relatively small. It is pointed out that the responses of story drift angle are able to be evaluated through the controlled displacement.

The maximum responses of drift angle at 1st story with Vop or Dcon during observed earthquake motions under different operation points of displacement restraint device are shown in Fig. 20. The relationships between Vop or Dcon and the story drift angles tend to be proportional.

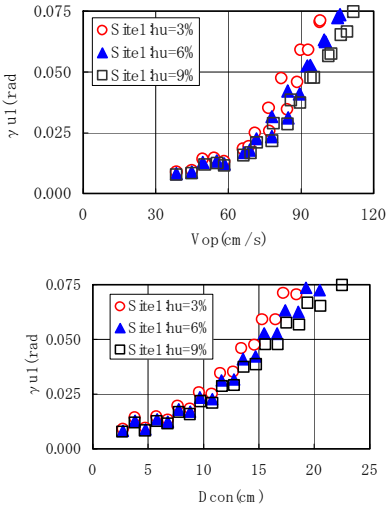

Fig. 21 Effect of damping ratios on story drift angles against simulated earthquake motions

Safety evaluation of houses with collision at isolated story

The effects of collision on response of drift angle at 1st story are discussed. The relationships between story drift angles and Vop or Dcon with different viscous damping ratios of superstructure during simulated earthquake motions are shown Fig. 21. Even if the isolated interface has the same condition of Vop or Dcon, the viscous damping ratios have some influence on decrease the story drift angles.

The relationships between story drift angles and the Dcon during observed earthquake motions are shown in Fig. 22. The effect of viscous damping ratios of superstructure expresses a similar tendency to the results in Fig. 21.

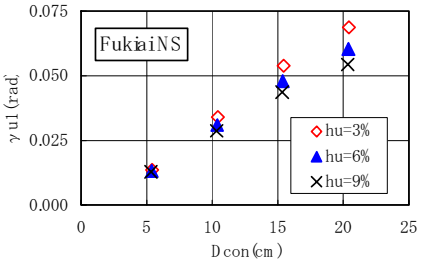

Fig. 22 Effect of damping ratios on story drift angles against observed earthquake motions

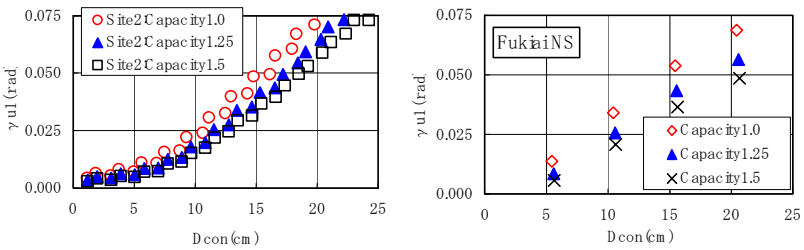

a) Simulated waves b) observed waves

Fig. 23 Effect of bearing capacity of superstructure on story drift angles against earthquake motions

The relationships between story drift angles and the Dcon with different bearing capacities of superstructure during earthquake motions are shown in Fig. 23. The effect of bearing capacities on the story drift angles is clearly shown. The response with 1.5 times of the bearing capacity is remarkably smaller than that with standard condition (bearing capacity: 1.0).

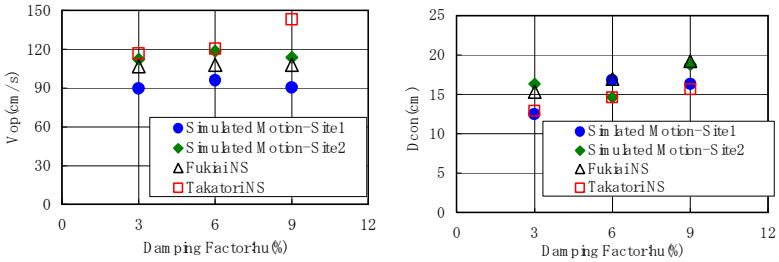

Fig. 24 Vop and Dcon at safety limit of superstructure with different viscous damping ratios

The Vop and Dcon where the story drift angles reach 0.005 (1/20) rad with different viscous damping ratios and different bearing capacities of superstructures are drawn in Figs. 24 and 25, respectively. The values of Vop and Dcon provide the limitation of collision condition where the safety of superstructures is kept against severe earthquake. In cases where the Vop exceeds 90 to 120 cm/s, the story drift angles will be probably larger than safety limit. The Vop is scattered with kinds of earthquake motions. On the other hand, the Dcon is less scattered and effects of viscous damping ratios and bearing capacities of superstructures on them tend to be much clear. In the design of isolated story against collision, the Vop and Dcon are very useful to check the safety of superstructures. Since the values of Vop and Dcon are dependent on the characteristics of isolators and displacement restraint device, more researches on effects of these characteristics on the response of superstructures are necessary.

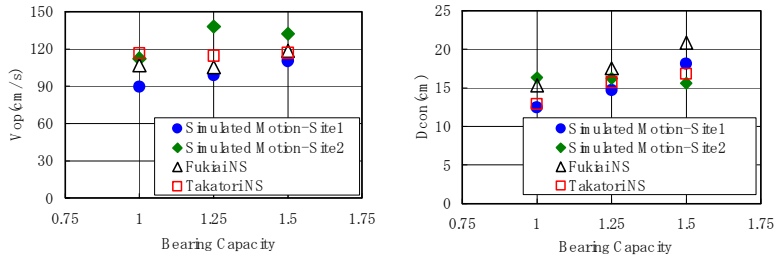

Fig. 25 Vop and Dcon at safety limit of superstructure with different bearing capacities

CONCLUSIONS

Shaking table tests are conducted to investigate the responses of the seismically isolated system with rubber bearings for houses and to verify the effect of displacement restraint device. In addition, the numerical analysis on earthquake response of base-isolated houses with displacement restraint device is conducted to obtain effects of displacement restraint devices with displacement-hardening type on story drift responses of superstructures. Concluding remarks are summarized as follows;

a) To improve the stability of load bearing capacity, steel plates which prevent rubber isolators from buckling are added. The rubber isolators with plates show very stable characteristics and the equivalent stiffness and equivalent damping ratios are little dependent on horizontal displacement.
b) The seismically isolated model provides remarkable decrease of acceleration response to input acceleration. In case during severe earthquakes, the collision occurs at the isolated interface. The acceleration response increases due to the collision.
c) The simulated results of isolated model have good agreements with those in the experiment. The shear coefficient of isolated interface during the collision in the analysis is a little larger than that in the experiment. Because it seems that the hysteretic damping of displacement restraint device is neglected in the analysis.
d) The story drift angle is the index of ultimate situation of superstructure and story drift angle are arranged by following two factors in the analysis; one is maximum velocity of isolated interface at the operation points (Vop), and the other is the controlled displacement (Dcon). The story drift angles remarkably increase with the amplitude of Vop or Dcon. In the design of isolated interface against collision, the Vop and Dcon are very useful to check the safety of superstructures.

ACKNOWLEDGEMENTS

The authors would like to express their sincere thanks to all the members of the committee on "Development of new technologies for seismic isolators for houses", the chairman of which is Dr. Shoichi Yamaguchi, president of Tokyo Kenchiku Structural Engineers, for providing data and valuable suggestions related to this study. The kind assistance of Dr. Keiichi Tamura, Public Work Research Institute in operating the shaking table is greatly appreciated.

REFERENCES

1. Iiba, M., Yamanouchi, H., Midorikawa, M., et al. "Research on performance of base isolated house", Proceedings of the Second World Conference on Structural Control, Kyoto, Vol.2, pp.1119-1126, 1998
2. Iiba, M., Midorikawa, M., Kawai, M., et al. "Shaking table tests on seismic behavior of isolators for houses", Proceedings of the 10th Japanese Earthquake Engineering Symposium, Yokohama, Japan, pp.2653-2658, 1998
3. Myslimaj, B., Midorikawa, M., et al. "Seismic behavior of a newly developed base isolation system for houses", Journal of Asian Architecture and Building Engineering, vol.1, No.2, pp. 17-24, 2002
4. Iiba, M., Midorikawa, M., Yamanouchi, H., et al. "Shaking table tests on performance of isolators for houses subjected to three dimensional earthquake motions", Proceedings of 12th World Conference of Earthquake Engineering, Auckland, Paper no. 1765, 2000
5. Midorikawa, M., Hiraishi, H., et al. "Development of Seismic Performance Evaluation Procedures in Building Code of Japan", Proceedings of 12th World Conference of Earthquake Engineering, Auckland, Paper no. 2215, 2000
6. Yoshida, N. and Suetomi, I. "DYNEQ: a computer program for dynamic analysis of level ground based on equivalent linear method, Reports of Engineering Research Institute, No. 22, Sato Kogyo Co., Ltd., pp.61-70, 1996 (in Japanese)
7. Ohsaki, Y., Hara, A., et al. "Stress-strain model of soils for seismic analysis", Proceeding of the 5th Japanese Earthquake Engineering Symposium, pp.679-704, 1978 (in Japanese)